

## VECTOR CLUSTERING OF PASSIVE MILLIMETER WAVE IMAGES WITH LINEAR POLARIZATION FOR CONCEALED OBJECT DETECTION

Seokwon Yeom<sup>\*</sup>, Dong-Su Lee, Hyoung Lee, Jung-Young Son, and Vladimir P. Guschin

Division of Computer and Communication Engineering, Daegu University, Gyeongsan, Gyeongbuk 712-714, Korea

**Abstract**—Passive millimeter (MMW) imaging can penetrate clothing to create interpretable imagery of concealed objects. However, the image quality is often restricted by low signal to noise ratio and temperature contrast as well as low spatial resolution. In this paper, we explore a four-channel passive MMW imaging system operating in the 8 and 3 mm wavelength regimes with linear vertical and horizontal polarization directions. Both registration between different channel images and segmentation of concealed objects are addressed. Multi-channel image registration is performed by geometric feature matching and affine transform, and then multi-level segmentation separates the human body region from the background, and concealed objects from the body region, sequentially. In the experiments, several metallic and non-metallic objects concealed under clothing are captured in indoors. It will be shown that our method can separate objects with higher accuracy than the conventional method.

### 1. INTRODUCTION

Millimeter wave (MMW) technology has been researched for wireless communication, radio astronomy, remote sensing, and imaging under low visibility conditions [1–3]. In recent years, the interest in passive MMW imaging technique has grown in the fields of security and defense [4–7]. Passive MMW imaging systems can penetrate clothing in order to identify concealed object [8, 9]. Passive MMW imaging largely depends on the temperature distribution of objects and their emissivity and reflectivity [5]. Since the received signal is usually a weak thermal

---

*Received 19 February 2013, Accepted 1 April 2013, Scheduled 23 April 2013*

<sup>\*</sup> Corresponding author: Seokwon Yeom (yeom@daegu.ac.kr).

signal, the sensitivity and noise robustness of the imaging system are crucial to the acquisition of high quality images. Compared with active imaging, passive imaging systems are free of speckle and glint, and can be built as stand-off type sensors. However, the image quality is often deteriorated by low signal-to-noise ratio and temperature contrast.

Image segmentation is the process by which foreground objects are separated from background regions [10]. A number of segmentation methods have been developed for detecting concealed objects on body region in MMW images. The EM algorithm is adopted to cluster pixels on the basis of a Gaussian mixture model in [11–13]. Multi-level thresholding has been introduced to detect the contours of the concealed objects in Terahertz (THz) images [14], while image segmentation using the Gaussian mixture model (GMM) has been applied to metallic object detection [15]. Recently, multi-level segmentation method is applied to segment a concealed object in the passive MMW image [16, 17].

In this paper, we investigate multi-channel image registration and multi-level segmentation of concealed objects. The images are obtained by the passive MMW imaging system equipped with four-channel receivers operating in the 8 and 3 mm wavelength regimes with linear vertical and horizontal polarization directions, thus the imaging system is capable of generating four images simultaneously. A registration process is required in order to combine different channel images into a multi-dimensional vector-per-pixel image. We combine different polarization images by mean of the registration process based on the edge detection and affine transform. The polarization direction is one of the factors deciding the image contrast, however the polarization effects on the target recognition have been seldom researched in the literature [5].

After the registration multi-level segmentation is applied to the vectors to segment any concealed objects. This multilevel segmentation implies two-level image segmentation. The body region is extracted from the background at the first (global) level of segmentation, and the concealed object region is segmented from the body area in the second (local) level of segmentation. Each level of segmentation comprises  $k$ -means clustering, and application of the expectation maximization (EM) algorithm and the Bayesian decision rule. The  $k$ -means clustering initializes the parameters (means, variances, and weights of the Gaussian mixture distribution (GMM)), and the EM algorithm iteratively estimates those parameters unto convergence [18]. The Bayesian decision rule assigns each pixel to a cluster of maximum posterior probability. In the experiments, several metallic and non-metallic objects such as knife, hand-axe, gun, rubber mallet, and

beauty-aid plastic bottle are captured in indoors. The results with multi-channel images are compared to those of the conventional method with a single-channel image.

The paper is organized as follows: in Section 2, we discuss the multi-channel passive MMW imaging system. Section 3 presents multi-level segmentation method with the registration of different polarization images. In Section 4, we present experimental results and some concluding remarks follow in Section 5.

## 2. MULTI-CHANNEL PASSIVE MILLIMETER WAVE IMAGING SYSTEM

The passive MMW imaging system is equipped with a Cassegrain dish antenna with a diameter of 0.5 m. Four feed horn antennas are located at the focal plane of the dish antenna receiving the regime of 8 mm and 3 mm wavelengths with linear vertical and horizontal polarization directions. Four receivers are connected to each feed horn individually, as illustrated in Figure 1. A receiver channel is composed of the wave guide, the Dicke receiver, three monolithic microwave integrated circuit (MMIC) amplifiers, and a Schottky diode detector. The scanning motors rotate both the antenna and the receiver in vertical and horizontal directions with a constant angular step for raster scanning. The angular resolution is around  $1.1^\circ$  and  $0.4^\circ$  according to the Rayleigh criterion when  $\lambda$  is 8 mm and 3 mm, respectively. The angular step size and the integrating time can be modified from  $0.1^\circ$  to  $1^\circ$  and from 20 ms to 200 ms, respectively.

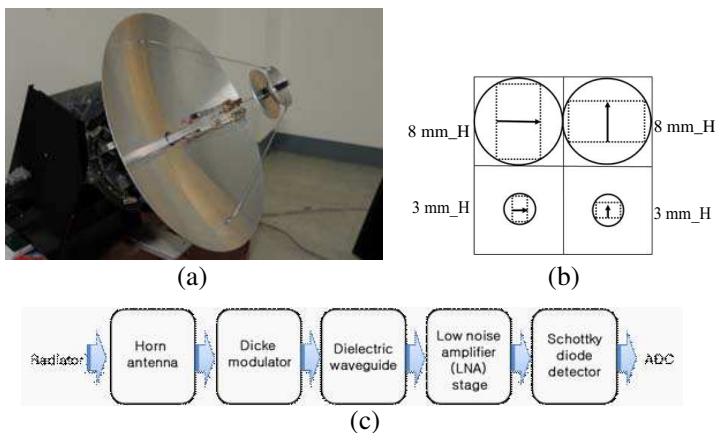


**Figure 1.** (a) Passive MMW imaging system, (b) four-channel configuration, (c) signal flow.

### 3. AUTOMATIC CONCEALED OBJECT DETECTION

The passive MMW imaging system operates in the 8 and 3 mm wavelength regimes with two linear polarization directions. The registration process is preceded to remove the geometrical discrepancy between different channel images, and then the concealed object detection is performed by the multilevel segmentation. The multilevel segmentation is composed of two-level image segmentation processes using  $k$ -means algorithm with splitting initialization, EM algorithm, and Bayesian decision rule as illustrated in Figure 2.

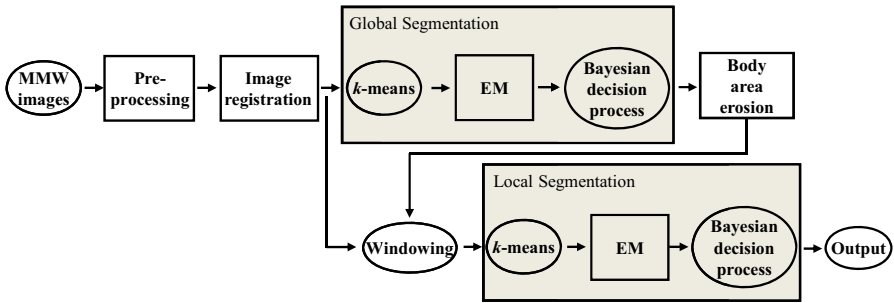


**Figure 2.** Block diagram of the concealed object detection.

#### 3.1. Multi-channel Image Registration

The registration process consists of feature extraction, feature matching, and affine transform [19]. The edge image is extracted by the Canny edge detection method. The maximum normalized correlation between two edge images estimates parameters such as rotation, scale, and translation. Figure 3 shows the overall procedure of the image registration.

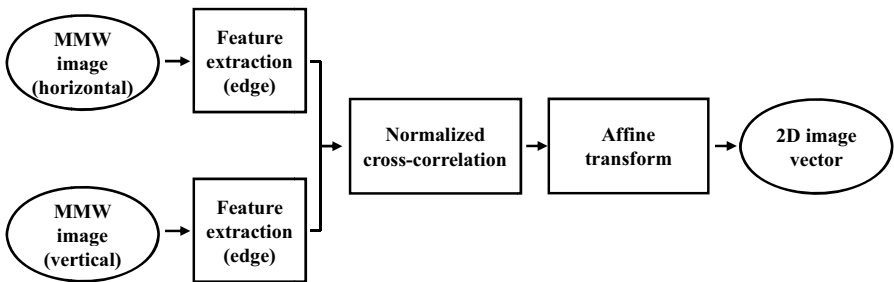


**Figure 3.** Block diagram of the image registration.

### 3.2. Multi-level Segmentation

This multilevel segmentation adopts  $k$ -means algorithm, EM algorithm for the GMM parameter estimation, and Bayesian decision rule. The  $k$ -means algorithm initializes the parameters of the GMM at each segmentation level. The EM process estimates the GMM parameters iteratively and the Bayesian decision rule decides which cluster each pixel belongs to. The first level EM extracts the body area from the background. The first Bayesian decision rule is followed by body area detection, which removes any segmented object inside the body area. During this process, we also perform the morphological erosion of the body area in order to estimate the accurate contour of the body area. The second level EM is followed by the second Bayesian decision rule to detect the concealed objects in the body area.

At each level of the EM process, the histogram is modeled with  $N_k$  components of the Gaussian distributions. The probability of density function of  $\mathbf{x}_t$  is assumed as

$$p(\mathbf{x}_t) = \sum_{k=1}^{N_k} N(\mathbf{x}_t | \boldsymbol{\mu}_k, \Sigma_k) P(G_k), \quad t = 1, \dots, N_t, \quad (1)$$

where  $\boldsymbol{\mu}_k$  is the mean vector,  $\Sigma_k$  the covariance matrix of the cluster  $G_k$ , respectively,  $N_k$  the number of clusters,  $N$  the Gaussian distribution, and  $N_t$  the number of pixels. The EM algorithm uses a set of training data to iteratively estimate the parameters  $\boldsymbol{\mu}_k$ ,  $\Sigma_k$  and  $P(G_k)$  until convergence. Figure 4 shows the block diagram of the EM algorithm;  $i$  represents the number of the iteration,  $\varepsilon$  and  $i_{\max}$  are the termination criteria for the iteration, and  $L_i$  is the likelihood  $L_i = \sum_{t=1}^{N_t} \log p_i(\mathbf{x}_t)$ . The following Bayesian decision rule assign pixels to one of  $N_k$  clusters:

$$j_t = \arg \max_{k=1, \dots, N_k} P(G_k | \mathbf{x}_t), \quad t = 1, \dots, N_t, \quad (2)$$

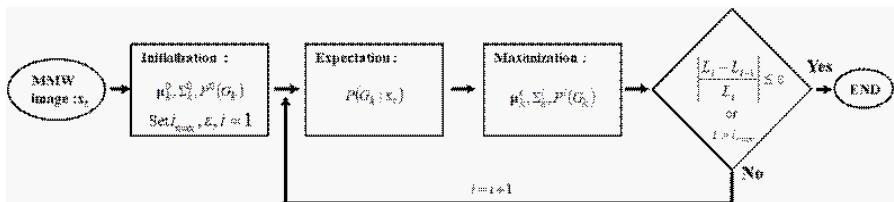


Figure 4. EM algorithm.

where

$$P(G_k|\mathbf{x}_t) = \frac{N(\mathbf{x}_t; \boldsymbol{\mu}_k, \Sigma_k) P(G_k)}{\sum_{k=1}^{N_k} N(\mathbf{x}_t; \boldsymbol{\mu}_k, \Sigma_k) P(G_k)}. \quad (3)$$

#### 4. EXPERIMENTAL AND SIMULATION RESULTS

A human subject hiding a metallic or non-metallic object is captured by the multi-channel passive MMW imaging system. The human subject faces the antenna 1.4m away from the system. The height of the human subject is around 176 cm. Figure 5 shows visible images of a human subject with concealment or without concealment. A knife with a wood grip, hand axe with a wood grip, and gun are attached to the human subject from left to right images in Figure 5. Figure 6



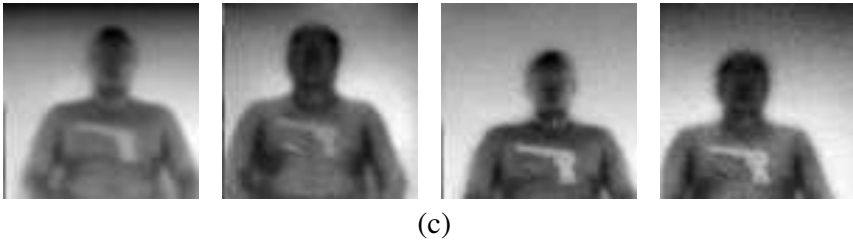
**Figure 5.** Visible images of a human subject with concealment and metallic objects: knife with a wood grip, hand axe with a wood grip, gun from left to right.



(a)



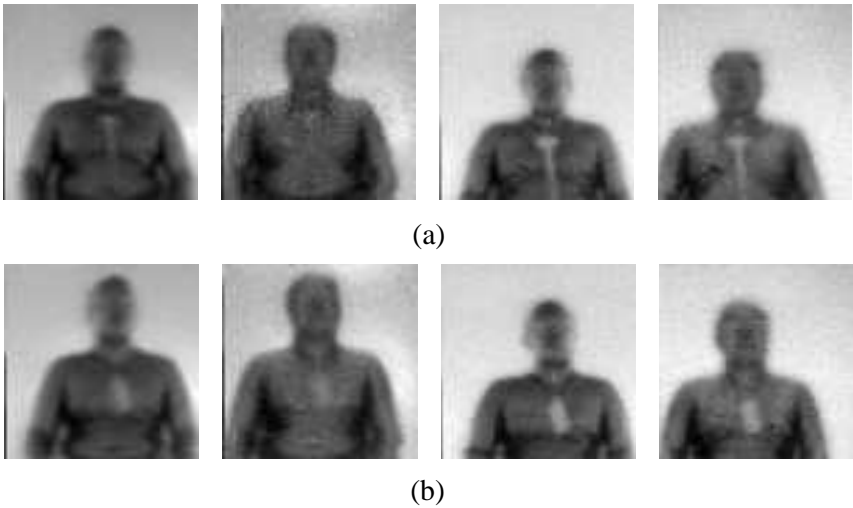
(b)



**Figure 6.** MMW images, 8 mm-V, 8 mm-H, 3 mm-V, 3 mm-H, from left to right, (a) knife, (b) hand axe, (c) gun.

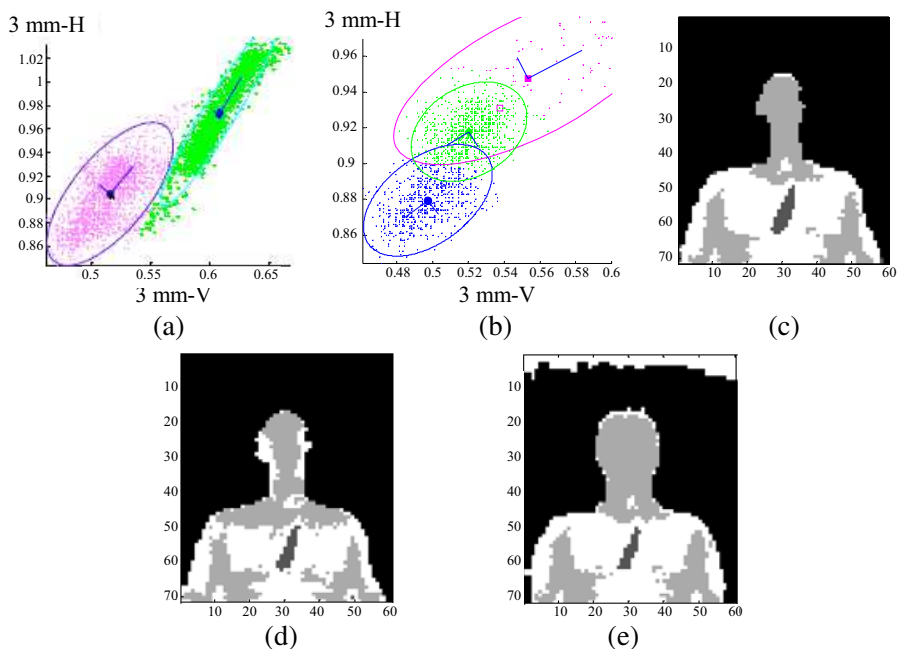


**Figure 7.** Non-metallic objects: rubber mallet with wood grip, plastic bottle containing beauty-aid liquid, from left to right.

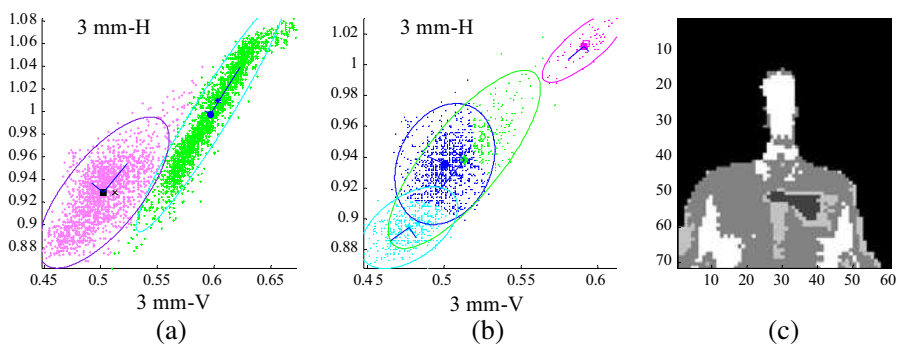


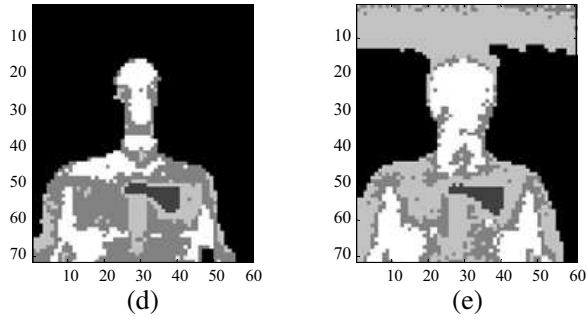
**Figure 8.** MMW image, 8 mm-H, 8 mm-V, 3 mm-H, 3 mm-V, from left to right, (a) rubber mallet, (b) plastic bottle.

shows the MMW images of three objects: 8 mm-V (vertical), 8 mm-H (horizontal), 3 mm-V, 3 mm-H images from left to right. The size of the passive MMW images is  $76 \times 75$  pixels. Figures 7 and 8 are the



**Figure 9.** Registration and segmentation results of 3 mm-H and 3 mm-V MMW images of a knife, (a) GMM distribution after global segmentation ( $N_k = 2$ ), (b) GMM distribution after local segmentation ( $N_k = 3$ ), (c) multi-channel segmentation, (d) single-channel segmentation (3 mm-V), (e) single channel segmentation (3 mm-H).

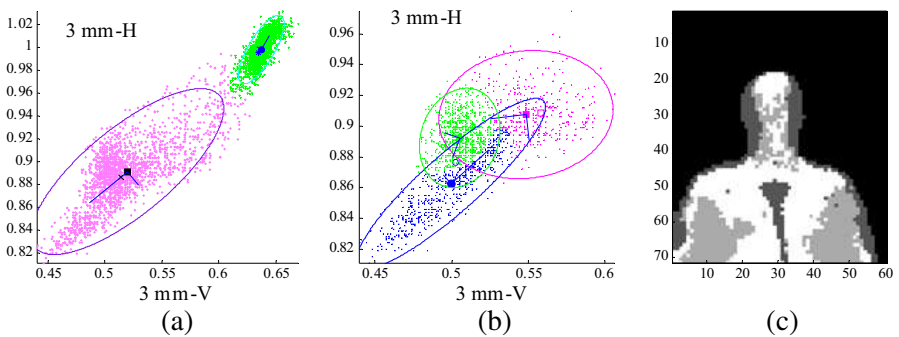




**Figure 10.** Registration and segmentation results of 3 mm-H and 3 mm-V MMW images of a hand axe, (a) GMM distribution after global segmentation ( $N_k = 2$ ), (b) GMM distribution after local segmentation ( $N_k = 4$ ), (c) multi-channel segmentation, (d) single channel segmentation (3 mm-V), (e) single channel segmentation (3 mm-H).

visible and MMW images of two non-metallic objects: rubber mallet with a wood grip, and plastic bottle containing beauty-aid liquid.

The segmentation is performed as two-dimensional vector clustering after registration between 3 mm-H and 3 mm-V images. Figures 9(a) and 9(b) show the GMM distribution after the global and the local segmentation, respectively. The number of clusters are set to 2 and 3. Figure 9(c) is the local segmentation results. Figures 9(d) and 9(e) show the single channel segmentation results with a 3 mm-V and a 3 mm-H image, respectively. Figures 10 and 11 are the results of hand axe and rubber mallet images, respectively. It is shown that the multi-channel results are more accurate than the single channel analysis. The top parts of Figures 9(e) and 10(e) are segmented as



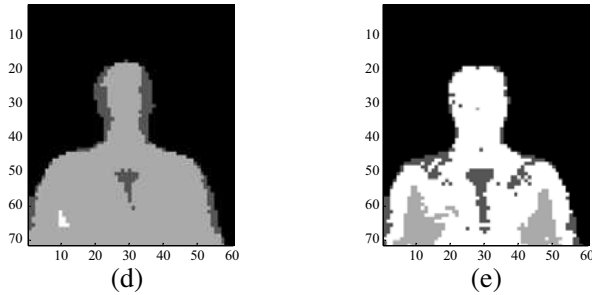


**Figure 11.** Registration and segmentation results of 3 mm-H and 3 mm-V MMW images of a rubber mallet, (a) GMM distribution after global segmentation ( $N_k = 2$ ), (b) GMM distribution after local segmentation ( $N_k = 3$ ), (c) multi-channel segmentation, (d) single channel segmentation (3 mm-V), (e) single channel segmentation (3 mm-H).

the parts of the body area. Figure 10(d) indicates that the segmented region is much bigger than the ground truth in the metal and grip parts. Figures 11(d) and 11(e) show that the single-channel method causes more errors than the multi-channel counterpart.

## 5. CONCLUSIONS

In this paper, we have presented the multi-channel image registration and multi-level segmentation techniques for concealed weapon detection. The images are captured by the multi-channel passive MMW imaging system operating four receivers simultaneously. The passive MMW images usually have the low contrast and resolution. The images are often noisy due to the low signal level. It has been shown that the segmentation results by multi-channels are more robust to noise and less sensitive to the background than the segmentation with the single channel image. We only utilize 3 mm measurements in this research. Further consideration for 8 mm measurements remains for the future study.

## ACKNOWLEDGMENT

This work was supported by the Daegu University research grant.

## REFERENCES

1. Zhang, J.-C., Y.-Z. Yin, and J.-P. Ma, "Design of narrow band-pass frequency selective surfaces for millimeter wave applications," *Progress In Electromagnetics Research*, Vol. 96, 287–298, 2009.
2. Mohammad-Taheri, M., M. Fahimnia, Y. Wang, M. Yu, and S. Safavi-Naeini, "Wave analysis for inductively matched millimeter wave amplifier design," *Progress In Electromagnetics Research C*, Vol. 13, 41–50, 2010.
3. Siles, G. A., J. M. Riera, P. Garcia-del-Pino, and J. Romeu, "Atmospheric propagation at 100 and 300 GHz: Assessment of a method to identify rainy conditions during radio soundings," *Progress In Electromagnetics Research*, Vol. 13, 257–279, 2012.
4. Chen, H.-M., S. Lee, R. M. Rao, M.-A. Slamani, and P. K. Varshney, "Imaging for concealed weapon detection: A tutorial overview of development in imaging sensors and processing," *IEEE Signal Processing Magazine*, Vol. 22, 52–61, 2005.
5. Kim, W.-H., N.-W. Moon, H.-K. Kim, and Y.-H. Kim, "Linear polarization sum imaging in passive millimeter-wave imaging system for target recognition," *Progress In Electromagnetics Research*, Vol. 136, 175–193, 2013.
6. Appleby, R. and R. N. Anderton, "Millimeter-wave and submillimeter-wave imaging for security and surveillance," *Proceedings of the IEEE*, Vol. 95, 1683–1690, 2007.
7. Yujiri, L., M. Shoucri, and P. Moffa, "Passive millimeter-wave imaging," *IEEE Microwave Magazine*, Vol. 4, 39–50, 2003.
8. Demirci, S., H. Cetinkaya, E. Yigit, C. Ozdemir, and A. Vertiy, "A study on millimeter-wave imaging of concealed objects: applications using back-projection algorithm," *Progress In Electromagnetics Research*, Vol. 128, 457–477, 2012.
9. Cooper, K. B., R. J. Dengler, N. Llombart, T. Bryllert, G. Chattopadhyay, I. Mehdi, and P. H. Siegel, "An approach for sub-second imaging of concealed objects using terahertz (THz) radar," *J. Infrared, Milli. Terahz Waves*, Vol. 30, 1297–1307, 2009.
10. Gonzalez, R. C., *Digital Image Processing 2/E*, Prentice-Hall Inc., 2003.
11. Delignon, Y., A. Marzouki, and W. Pieczynski, "Estimation of generalized mixtures and its application in image segmentation," *IEEE Trans. on Image Processing*, Vol. 6, No. 10, 1364–1375, 1997.

12. Farnoosh, R. and B. Zarpak, "Image segmentation using Gaussian mixture model," *IUST Int. J. Engineering Science*, Vol. 19, 29–32, 2008.
13. Comer, M. L. and E. J. Delp, "Segmentation of textured images using a multiresolution Gaussian autoregressive model," *IEEE Trans. on Image Processing*, Vol. 8, 408–420, 1999.
14. Shen, X., C. R. Dietlein, E. Grossman, Z. Popovic, and F. G. Meyer, "Detection and segmentation of concealed objects in Terahertz images," *IEEE Trans. on Image Processing*, Vol. 17, 2465–2475, 2008.
15. Haworth, C. D., Y. De Saint-Pern, D. Clark, E. Trucco, and Y. R. Petillot, "Detection and tracking of multiple metallic objects in millimeter-wave images," *International Journal of Computer Vision*, Vol. 71, 183–196, 2007.
16. Yeom, S., D.-S. Lee, J.-Y. Son, M.-K. Jung, Y. Jang, S.-W. Jung, and S.-J. Lee, "Real-time outdoor concealed-object detection with passive millimeter wave imaging," *Opt. Express*, Vol. 19, 2530–2536, 2011.
17. Yeom, S., D.-S. Lee, and J.-Y. Son, "Multi-level segmentation of passive millimeter wave images for hidden object detection," *Optical Engineering*, Vol. 51, 091613, 2012.
18. Bishop, C. M., *Neural Networks for Pattern Recognition*, Chap. 2, Oxford, 1995.
19. Lee, H., D.-S. Lee, S. Yeom, J.-Y. Son, V. P. Guschin, and S.-H. Kim, "Image registration and fusion between passive millimeter wave images and visual images," *Journal of the Korean Institute of Communications and Information Sciences*, Vol. 36, 349–354, 2011.